Controlling the Conformation Changes Associated to Electron Transfer Steps through Chemical Substitution: Intriguing Redox Behavior of Substituted Vinylogous TTF

N. Bellec,[1a] K. Boubekeur,[1b] R. Carlier,[1a] P. Hapiot,*,†,[1c] D. Lorcy,*,[1a] and A. Tallec[1a]

Synthèse et Electrosynthèse Organiques, UMR CNRS 6510, Université de Rennes 1, campus de Beaulieu, 35042 Rennes Cedex, France, Laboratoire de Chimie des Solides, Institut des Matériaux de Nantes, 2 rue de la Houssinière, 44072 Nantes, France, and Laboratoire d'Electrochimie Moléculaire de l'Université Denis Diderot-Paris 7, UMR CNRS 7591, 2 place Jussieu, Case courier 7107, 75251 Paris Cedex 05, France

Received: April 6, 2000; In Final Form: July 13, 2000

Oxidation of a series of TTF vinylogues has been investigated in acetonitrile and dichloromethane. Depending on the substituent and the solvent, two single-electron transfers or one two-electron process was observed. Density functional modeling calculations and detailed analysis of the electrochemical behavior show that the unusual redox behavior for short-length TTF vinylogues is due to substantial conformation changes concerted with the electron transfers. Flash photolysis and spectroelectrochemistry experiments were also performed to confirm this conclusion. Through fine-tuning of the molecule structure and substituent choice, it is possible to control the relative stabilities of the different redox species. At one end, this leads to situations where the second electron transfer is much easier than the first one. At the other end, opposite situations are observed with a large increase of the separation between the first and second oxidation potentials by comparison to similar TTF without steric hindrance. The inner sphere reorganization energies remain modest (0.35−0.45 eV), allowing a fast passage between the different conformations during the electron transfers.

Introduction

Within the numerous modifications performed on the tetrathiafulvalene (TTF) core for the preparation of organic conductors, the introduction of one vinyl spacer between the dithiole rings has been the subject of several investigations.[2] Both donors TTF and their vinylogous analogues are known to be planar, but compared to the basic TTF framework, vinylogous TTF exhibit better donating properties with a smaller difference between the two oxidation potentials.[3] In this field, the preparation of substituted vinylogous TTF by oxidative coupling of 1,4-dithiafulvenes has attracted a lot of attention due to the ability of this method to introduce different substituents.[4−10] The addition of bulky substituents on the central conjugation moiety prevents the donor from being planar due to steric interactions.[5a,6,7,11] This nonplanarity takes nothing away from the donor ability of these derivatives, but an intriguing feature is their redox behavior. Indeed, depending on the substitution of the conjugated spacer group, one can observe by cyclic voltammetry either a reversible bielectronic transfer leading directly to the dicationic state or two reversible monoelectronic transfers corresponding to the consecutive formation of the radical cation and of the dication. This result is in contrast with the behavior of short-length TTF vinylogues which generally exhibit two monoelectronic transfers.[2] Essentially because of Coulombic interactions, the oxidation (or reduction) of organic molecules proceeds generally in a series of one-electron steps in which the removal of a second electron is more difficult than the first one.[12] This situation has been called normal ordering of potential and is the most common observation for the electrochemical reactions of organic molecules when the initially produced intermediates are chemically stable. In TTF series, it has been shown that the difference between the first and the second oxidation potentials can be reduced considerably by increasing the length of the conjugated spacer.[13] However, for the investigated family of molecules (see Chart 1), the conjugated spacer (with only one vinyl bond) is not long enough to explain the observed behavior by a simple decrease of the Coulombic interaction. Another hypothesis can be proposed on the basis of literature results.[12] Several experimental examples of "potential inversion" for the oxidation (or reduction) of short organic molecules have been reported when at least one of the electron transfers is associated with important structural changes.[12,14,15] When the information about the structures of the intermediates was available, on the basis of detailed analysis

CHART 1. General Formula of the Investigated TTF Vinylogues

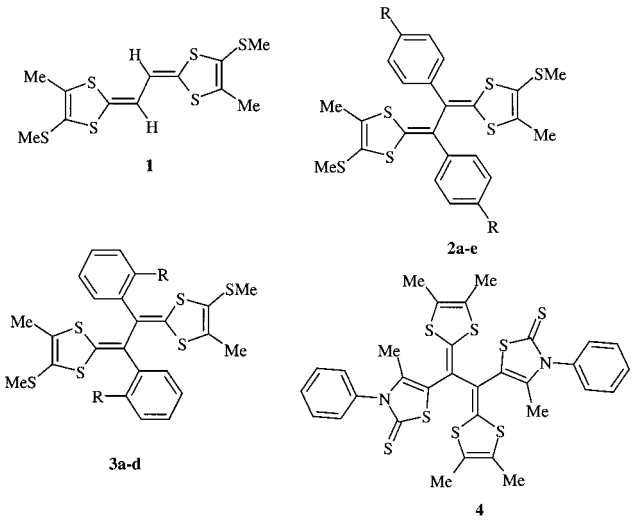

† Email: hapiot@paris7.jussieu.fr. Fax: +33 1 44 27 76 25.

10.1021/jp001326x CCC: $19.00
Published on Web 10/05/2000

of the electrochemical responses and by comparison with semiempirical AM1 calculations, D. H. Evans et al. have shown that the structural changes were the cause of potential inversion.[14,15a] Concerning the substituted vinylogous TTF, we have also observed considerable conformational modifications between the neutral and the dicationic states,[5a,16] in agreement with more recent observations.[6b] By analogy with literature reports concerning the inverted potentials,[12,14,15] we suggest that the unusual redox behavior observed for some of these short vinylogous TTF is related to structural changes induced by the steric interactions. However, in the framework of this hypothesis, the variation of the relative order of the potentials remains unclear. For example, situations of normal order of potentials or, on the contrary, of inverted potentials are observed for molecules belonging to the same family for which the steric constraints are expected to be similar.[6b,16a] Thus, it is of interest to rationalize the effects in order to control the conformational changes occurring during the electron transfer by a fine-tuning of the molecule structure through chemical substitution. In addition to the interest in these molecules for the engineering of new functional materials, the significant likelihood of chemical substitutions on the TTF core offers a unique route for a systematic investigation of multielectronic transfer associated with substantial conformational changes. In this paper, detailed studies of the electrochemical behavior of vinylogous TTF have been performed under the same experimental conditions. Crystallographic structures have been obtained for several derivatives, and molecular modelings based on density functional theory (DFT) have been performed to understand and control the evolution of the phenomenon as a function of the substitution. The electron transfers have been studied for the following families of donors: the unsubstituted **1** which serves as a reference compound, TTF vinylogues with phenyl groups substituted on their para or ortho positions (respectively **2a**−**e** or **3a**−**d**) by different donating or withdrawing substituents and with thiazole groups **4** that change both the steric hindrance and the electronic properties.

Experimental Section

Chemicals. All of the vinylogous tetrathiafulvalenes (TTF) have been prepared by oxidative dimerization of 1,4-dithiafulvenes in a one-pot procedure by a two-step electrochemical synthesis: first an oxidation of the monomer and then a reduction of the solution.[5] Acetonitrile was Uvasol quality (Merck). Dichloromethane was Rectapur quality (Prolabo). The supporting electrolytes NEt_4BF_4 and NBu_4BF_4 were from Fluka (puriss quality). Solutions were prepared freshly before experiments and oxygen was removed by bubbling argon.

Electrochemical Experiments. All of the cyclic voltammetry experiments were carried out at 20 ± 0.1 °C using a cell equipped with a jacket allowing circulation of water from the thermostat. The counter electrode was a Pt wire and the reference electrode an aqueous saturated calomel electrode with a salt bridge containing the supporting electrolyte. The SCE electrode was checked against the ferrocene/ferricinium couple (considering the following $E°$ values: $E° = +0.405$ V/SCE in acetonitrile and +0.528V/SCE in dichloromethane) before and after each experiment. Based on repetitive measurements, absolute errors on potentials were found to be around ±5 mV. In situations of inverted potentials, ΔE_p measurements (which do not require the standardization of the reference electrode) were repeated at least 10 times and averaged. Errors were found to be ±1mV.

For low scan rate cyclic voltammetry (0.05−500 V s^{-1}), the working electrode was a 1 mm diameter platinum disk (or glassy carbon disk made from a 3 mm diameter cylinder from Tokai Corp. or a 1 mm diameter gold for test experiments). It was carefully polished before each set of voltammograms with 1 μm diamond paste and ultrasonically rinsed in absolute ethanol. Electrochemical instrumentation consisted of a PAR model 175 universal programmer and of a home-built potentiostat equipped with a positive feedback compensation device.[17] The data were acquired with a 310 Nicolet oscilloscope.

For high scan rate cyclic voltammetry, the ultramicroelectrode was a platinum wire (10 μm diameter) sealed in soft glass.[18] The signal generator was a Hewlett-Packard 3314A and the curves were recorded with a 4094C Nicolet oscilloscope with a minimum acquisition time of 5 ns per point.

Spectroelectrochemical experiments (spectrovoltammetry) were performed with a capillary-slit-cell for UV−visible spectroscopy using gold−LIGA structures (100 μm thickness) as an optical transparent electrode. The equipment was described in previously published papers.[19] The complete electrochemical conversion in the capillary slit occurs in less than two seconds.

Numerical simulations of the voltammograms were performed with the commercial BAS Digisim Simulator 2.1[20] using the default numerical options with the assumption of planar diffusion. The Butler−Volmer law was considered for the electron-transfer kinetics (see text). The coefficient, α, was taken as 0.5 and the diffusion coefficients equal for the all the species ($D = 10^{-5}$ cm^2 s^{-1}).

Flash Photolysis Experiments. Irradiations were performed with a Questek laser 2048 (100−150mJ/20−50ns) using a XeCl mixture ($\lambda = 308$ nm). The detection system consisted of a 150-W xenon lamp, a 1.5 cm optical path length irradiation cell, a SP 150 spectrograph (ARC), and an intensified diode array system (PG200 pulsed generator, ST-121 controller and IRY-700 S/RB detector from Princeton Instruments, Inc). For the acquisition, the pulse width was set to 100 ns, and the delay after the laser pulse was adjusted to be as short as possible to avoid the observation of laser flash. Spectra were averaged 10 times to improve the signal-to-noise ratio.

Theoretical Modeling. The calculations were performed using the Gaussian 98 package[21] for density functional and solvation calculations. Gas-phase geometries and electronic energies were calculated by full optimization without imposed symmetry of the conformations using the B3LYP[22] density functional with the 6-31G* basis set,[23,24] starting from preliminary optimizations performed with semiempirical methods. Because of the difficulty to run frequency calculations with the large investigated molecules, the quality of the obtained minima were checked by restarting the optimizations from other conformations, which led to the same optimized geometries. Solvation free energies were calculated on the gas-phase optimized conformations according to the SCRF (self-consistent reaction field) method using the IPCM method[25] and the B3LYP density functional. In this method, the solvent is treated as a continuum of uniform dielectric constant in which the solute is placed into a cavity defined as an isodensity surface of the molecules. The value for the isodensity surface was chosen as 0.001 electrons/$bohr^3$, as used in previous published calculations.[25a] For solvent reorganization energy, $\lambda_{0,elec}$, estimations, the radii of the equivalent spheres of the various species of interest were obtained by means of a volume calculation on the optimized geometries, meaning the volume inside a contour of 0.001 electrons/$bohr^3$ density.

Results and Discussion

Cyclic Voltammetry Experiments. Investigations of the vinylogous TTF oxidation were performed in acetonitrile and

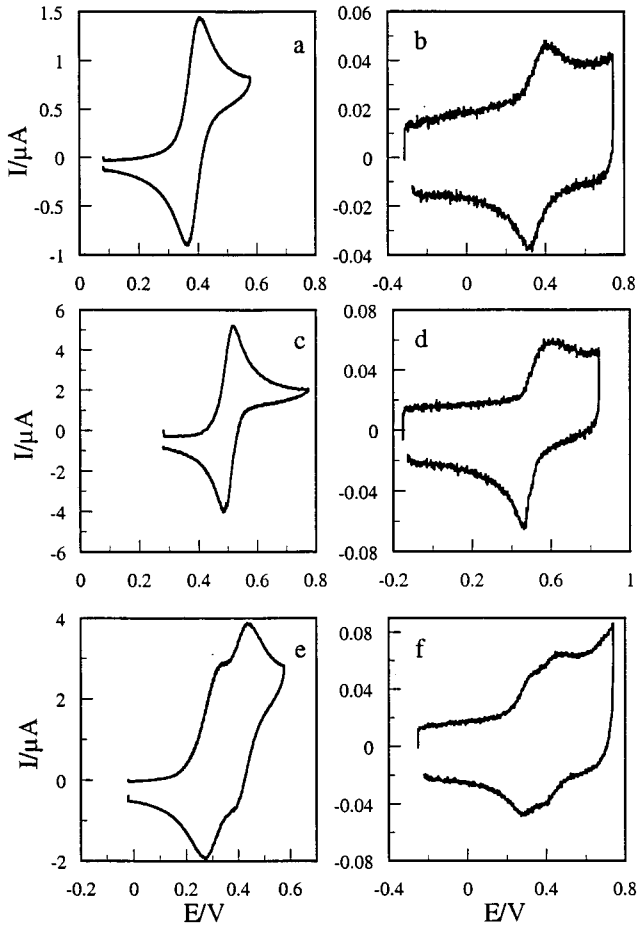

Figure 1. Cyclic voltammetry of the TTF vinylogues oxidation on a 1 mm Pt electrode (a, c, e) or a 10 μm ultramicrolectrode (b, d, f) in acetonitrile + 0.1 mol L^{-1} NEt_4BF_4. Scan rates: 0.2 V s^{-1} (a, c, e), 1000 V s^{-1} (b, d, f). **2d** (R=p$MeOC_6H_4$) (a, b), **2b** (R=pNCC_6H_4) (c, d), **1** (R=H) (e, f). Conc = 6×10^{-4} (a,b), 4.5×10^{-4} (c,d), 8.5×10^{-4} mol L^{-1} (e,f).

SCHEME 1

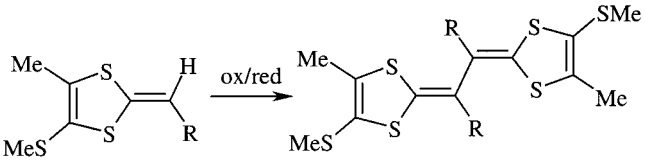

in dichloromethane for the compounds reported in Scheme 1 using cyclic voltammetry on a platinum electrode. We checked that the same behavior is observed when changing the nature of the working electrode (glassy carbon). As illustrative examples, typical voltammograms for the nonsubstituted compound **1** and two vinylogous TTF **2b**, **2d** bearing bulky substituents on the central core are displayed in Figure 1 at two different scan rates 0.1 and 1000 V s^{-1} in acetonitrile. Oxidation waves were always reversible, but, depending on the substituent and on the solvent, two single-electron transfers or one two-electron process was observed. For the vinylogous TTF substituted by the aromatic groups (e.g., **2a**−**e**), only one reversible oxidation wave associated with the concomitant exchange of two electrons was observed in acetonitrile. In the investigated time-window (0.05−5,000 V s^{-1}), no other intermediate that can be detected through a new redox process was observed. The main modification when raising the scan rates was an increase of the potential separation between the anodic (E_{pa}) and cathodic (E_{pc}) peaks. For compounds **2a** and **2b**, the anodic peak current becomes broader than the cathodic one, indicating an influence of the electron transfer kinetics (see below). From these reversible voltammograms recorded at low scan rate, it is immediately possible to derive the overall formal potential for the two-electron process $E^\circ_{2e^-} = (E^\circ_1 + E^\circ_2)/2$ as the half-sum between the two peak potentials $E^\circ_{2e^-} = (E_{pa} + E_{pc})/2$.[26] As calculated before,[27] if we assumed that the thermodynamics of both electron transfers is reached, the potential peak separation $\Delta E_p = E_{pa} - E_{pc}$ allows the measurement of the difference in standard (formal) potentials $\Delta E^\circ = E^\circ_2 - E^\circ_1$ (see the working curve in the supplementary section). For an infinite separation, ΔE_p tends to 28.25 mV at 20 °C, meaning that the measurement of the individual potentials becomes very inaccurate (then impossible) for large inversions of potential. The extracted ΔE°, assuming a thermodynamic control of the electron transfers, are gathered in Table 1 with the corresponding errors (see experimental part). The first observation is the clear inversion of the individual reversible formal potentials for the two steps, with the second electron being more easily removed than the first one. This peculiar behavior of substituted vinylogous TTF differs from the nonsubstituted compound **1** where a two-step process is involved (Table 1), in agreement with previously published results.[2] The second noticeable point is that the inversion of the individual formal potentials is larger when a withdrawing group is present on the phenyl ring, although a similar steric hindrance is expected for all of the molecules **2a**−**2e**.

To check the conclusions of Table 1, the oxidation steps were also followed by spectrovoltammetry during a full cycle scan of potential (the UV−visible spectra are recorded as functions of the applied potential in full conversion conditions) using as an optical transparent electrode a gold−LIGA electrode for three chosen compounds: the unsubstituted **1** and the substituted TTF **2b**, **2d** bearing respectively withdrawing and donor substituents. As seen in Figure 2, the spectrum of the electrogenerated radical-cation (large peak around 600 nm and absorbance in the 700−850 nm range) is clearly visible before the formation of the dication (only one peak around 580 nm) in the case of **1** and **2d**. On the contrary, the dication is produced directly during the oxidation of **2b**. It is clear that the radical cation is more visible in the case of **1** than for **2d**. Because the stability of the radical cation is directly related to ΔE°,[28] these results confirm the trend of Table 1, i.e., ΔE° for **1** > ΔE° for **2d** > ΔE° for **2b**. When a substituent is introduced on the ortho position of the phenyl group (compounds **3a**−**d**), a similar decrease of ΔE° is observed as a function of the withdrawing strength of the substituent. However, the extracted ΔE° are always larger for the ortho substituted molecules **3a**,**b**,**d** than for the corresponding para substituted molecules **2a**,**b**,**d**. Similar trends were found in dichloromethane. The use of this solvent instead of acetonitrile induced an increase of ΔE° for all investigated TTF. The effect is directly observable for compounds **2c**−**e**, **3b**, and **4**, which display two distinct monoelectronic waves in CH_2Cl_2 by contrast with a single bielectronic wave in CH_3CN. Actually, depending on the donating ability of the phenyl group, the bielectronic waves can split or not into two monoelectronic ones, but the same general effect was observed for all of the TTF in both solvents.

X-ray Structural Investigations. The molecular structure of the neutral donor **2d** determined by single-crystal X-ray analysis revealed a non planar geometry due to steric hindrance.[5a] This severely distorted structure has been found for all of the substituted TTF vinylogues,[6,7,11] even when R = Me.[6b] We recently reported dicationic salts of type **2** by simply mixing a

TABLE 1: Oxidation Potentials of TTF Vinylogues

		CH_3CN		CH_2Cl_2	
	R	$E^\circ_{2e^-}$/V (ΔE_p in mV)[a]	$\Delta E^\circ = E^\circ_2 - E^\circ_1$/mV[b]	$E^\circ_{2e^-}$/V (ΔE_p in mV)[a]	$\Delta E^\circ = E^\circ_2 - E^\circ_1$/mV[b]
1	H	0.321(57) 0.436(57)	115 ± 2	0.398(56) 0.579(57)	181 ± 2
2a	p-$NO_2C_6H_4$	0.546(31)	−65 ± 25	0.671(34)	−30 ± 10
2b	p-NCC_6H_4	0.530(30)	−90 ± 30	0.651(35)	−25 ± 6
2c	C_6H_5	0.413(37)	−13 ± 5	0.519(104)[c]	76 ± 1
2d	p-$MeOC_6H_4$	0.378(41)	4 ± 1	0.468(143)[c]	104 ± 2
2e	p-$Me_2NC_6H_4$	0.309(41)	4 ± 1	0.334(60) 0.454(61)	120 ± 2
3a	o-$NO_2C_6H_4$	0.467(92)	67 ± 1	0.495(57) 0.716(63)	221 ± 3
3b	o-NCC_6H_4	0.519(109)	79 ± 2	0.551(57) 0.767(70)	216 ± 3
3d	o-$MeOC_6H_4$	290(56) 402(59)	112 ± 2	0.293(59) 0.551(63)	258 ± 3
4	thiazoline thione	0.451(115)[c]	84 ± 2	0.532(61) 0.668(59)	136 ± 2

[a] Scan rate = 0.1 V s^{-1}. [b] Assuming an infinitively fast electron-transfer kinetics. [c] Double wave ($\Delta E_p = E_{pa2} - E_{pc1}$).

TABLE 2: Bond Lengths (Å) of Substituted Vinylogous TTF Core Obtained by X-ray Analyses

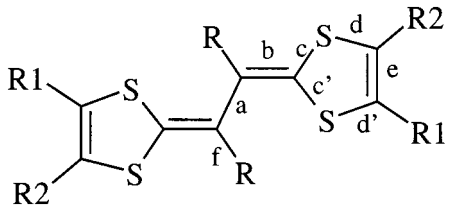

	neutral		radical cation			dication	
R =	2,6-$F_2C_6H_5$[a] R^1=R^2= SCH_2CH_2S	p-$MeOC_6H_4$[b] R^1=CH_3 R^2=SCH_3	o-ClC_6H_4[a] R^1=R^2= $(CH{=}CH_2)_2$	2,6-$F_2C_6H_5$[a] R^1=R^2= $(CH{=}CH_2)_2$	thiazoline[c] R^1=R^2= CH_3	p-$MeOC_6H_4$[b] R^1=CH_3 R^2=SCH_3	C_6H_5[b] R^1=CH_3 R^2=SCH_3
a	1.481(8)	1.469(9)	1.38(2)	1.41(1)	1.37(2)	1.371(4)	1.341(12)
b	1.354(6)	1.324(10)	1.417(13)	1.400(8)	1.44(2)	1.447(3)	1.462(8)
c	1.755(4)	1.762(7)	1.724(9)	1.725(6)	1.730(11)	1.695(2)	1.703(6)
c′	1.758(4)	1.781(8)	1.736(9)	1.725(7)	1.695(11)	1.689(2)	1.679(6)
d	1.747(4)	1.759(9)	1.750(2)	1.737(7)	1.727(12)	1.696(3)	1.690(6)
d′	1.755(4)	1.792(9)	1.730(8)	1.742(6)	1.727(13)	1.714(2)	1.722(6)
e	1.389(6)	1.339(11)	1.337(11)	1.394(9)	1.31(2)	1.366(3)	1.364(9)
f	1.483(5)	1.482(10)	1.56(2)	1.498(8)	1.49(2)	1.496(3)	1.504(9)

[a] From ref 6b. [b] From our ref 16b. [c] This work, $\mathbf{4}^{\bullet+}$.

solution of **2d** in CH_2Cl_2 with a solution of $Cu(ClO_4)_2 \cdot 6H_2O$ in THF or by exposing a solution of **2c** in CH_2Cl_2 to an iodine atmosphere.[16] In both cases, the vinylogous TTF in its dicationic form adopts a new conformation with a planar extended TTF core, whereas the phenyl groups are located in a perpendicular plane. Compound **4** was oxidized under the same conditions as used for **2c**. The 1:1 stoichiometry of the complex (one vinylogous TTF for one counterion) determined from X-ray structure analyses[29] implies that the TTF in this salt is in its cation radical state, $\mathbf{4}^{\bullet+}$. The radical cation and the dication display similar conformations with a planar TTF skeleton. Yamashita et al. have also lately reported similar observations on cation radical salts of vinylogous TTF substituted by bulky groups.[6] Despite their conformational changes, the bond length modifications of **2** depending on the oxidation state are similar to the ones observed for the nonsubstituted analogues **1**.[2g] To exemplify these changes, we summarized in Table 2 our results and the X-ray data from literature (Tables 2 and 3). Even if it is not possible to get the X-ray structures of all the redox states for the same compound, global examination of the results suggests that the major conformational modifications occur between the neutral and the cation radical state. Upon oxidation, the main modifications are observed on the conjugated system

TABLE 3: Bond Lengths (Å) of Unsubstituted Vinylogous TTF Core[a]

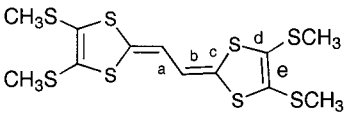

a

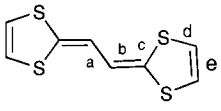

b

	neutral		radicalcation		dication
	crystal	B3LYP	crystal	B3LYP	B3LYP
a	1.434(5)	1.44	1.402(9)	1.40	1.36
b	1.355(4)	1.36	1.380(6)	1.40	1.45
c	1.749(3)	1.79	1.713(4)	1.75	1.71
c′	1.758(3)		1.739(4)		
d	1.749(3)	1.76	1.741(5)	1.74	1.72
d′	1.755(3)		1.746(4)		
e	1.346(4)	1.34	1.351(7)	1.35	1.36

[a] Experimental X-ray data (from ref 1g) for molecule a and B3LYP/6-31G* calculations for molecule b.

$S_2C{=}C{-}C{=}CS_2$. For instance, the central C−C bond (**a**) is lengthened while the two other C−C bonds (**b**) and the S−C bonds of the dithiole rings are shortened when compared with the neutral molecule. However, almost no significant changes

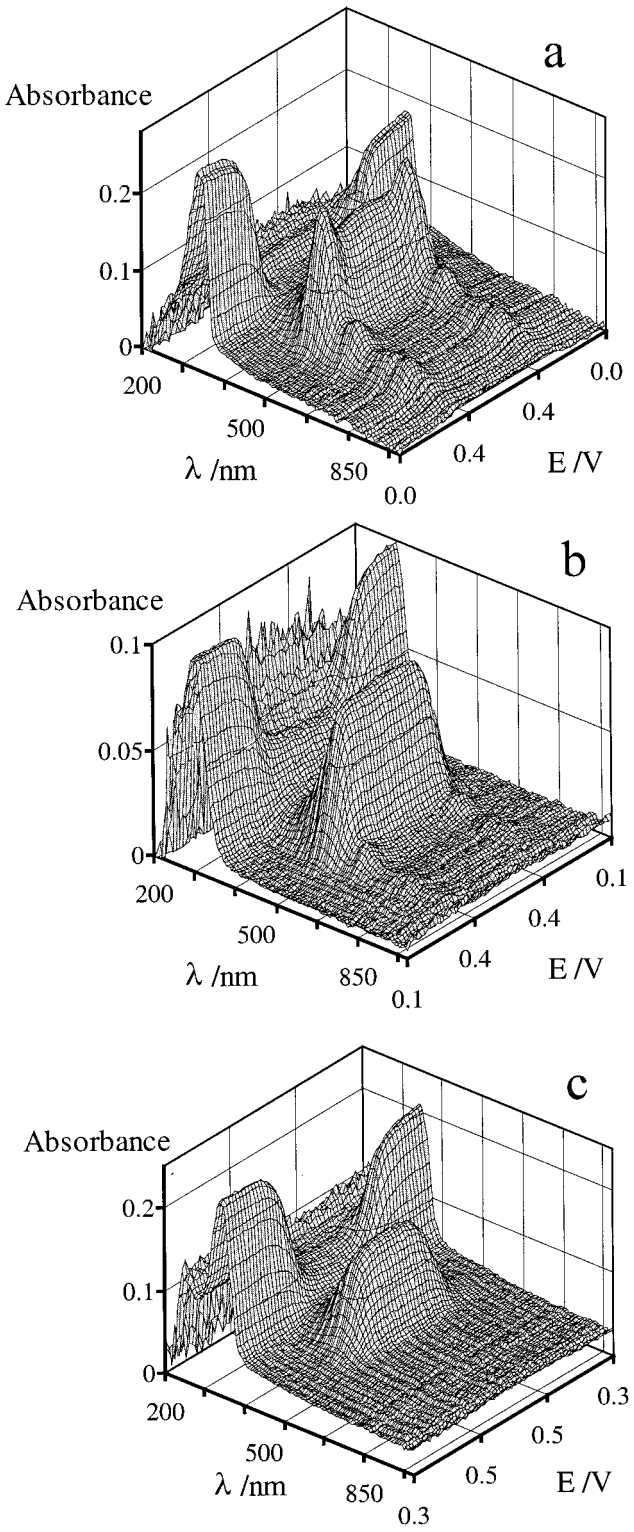

Figure 2. Spectroelectrochemistry of the oxidation of the TTF vinylogues in acetonitrile (+ 0.1 mol L^{-1} NEt_4BF_4). (a) **1** C° = 9 × 10^{-4} mol L^{-1}. (b) **2d** C° = 3.5 × 10^{-4} mol L^{-1}. (c) **2b**, C° = 4 × 10^{-4} mol L^{-1}. Scan rate = 0.05 V s^{-1}. (The reverse potential is located at the middle of the potential scale).

are detected on the bond (**f**), which linked the aryl group to the conjugated system.

Molecular Modeling. As explained in the Introduction, large structural changes can be responsible for a potential inversion for a two-step process in cases where the first electron transfer results in a species that is easier to oxidize than the original one.[12] By analogy with literature results and from the crystallographic data, we suggest that the unusual redox behavior for the TTF vinylogues is related to the observed structural changes. More surprisingly is the way that the oxidation potential separations $\Delta E°$ vary with the substitution. To rationalize the effects, we performed a series of molecular modeling calculations to determine both the geometry and the stability of the TTF vinylogues in their three oxidation states. This type of calculation also provides information on the molecular geometries when data are not available from the X-ray experiments. This is especially the case when the two-electron transfers are simultaneous, meaning that the radical cation is not stable versus its disproportionation.

TABLE 4: Bond Lengths (Å) of Phenyl-Substituted Vinylogous TTF Core Obtained by DFT Calculations at the B3LYP/6-31G* Level

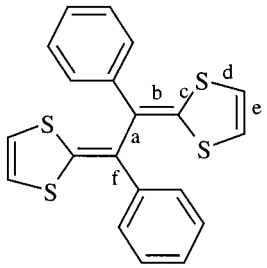

	neutral	radical cation	dication
a	1.50	1.42	1.38
b	1.36	1.41	1.46
c	1.79	1.76	1.72
d	1.76	1.74	1.72
e	1.34	1.35	1.36
f	1.49	1.50	1.50

The geometries of the neutral, radical cation, and dications were determined by a full optimization of the conformation using the B3LYP[22] density functional[23] as a compromise between precision and calculation time.[24] We made these calculations for five of the phenyl-substituted TTF vinylogues bearing the phenyl group with no substituent **2c**, with para **2b**, (R=p-NCC_6H_5), **2d** (R=p-$MeOC_6H_5$) or ortho substituents **3b** (R=o-NCC_6H_5), **3d** (R=o-$MeOC_6H_5$). Results for the unsubstituted TTF vinylogue **1** are collected in Table 3 and for the substituted ones in Table 4. To decrease the length of the calculations, the thiomethyl and methyl substituents on the dithiole rings were also omitted. For **1**, the neutral, radical cation and dication were found to be planar, in agreement with the known results for this compound. As expected, upon oxidation the central bond (**a**) shortens as the adjacent bond (**b**) increases, showing the passage of the double bond characters from the (**a**) to (**b**) position. For the phenyl-substituted compound **2c**, the situation is different (see Table 4 and Figure 4). In the radical cation and the dication, the TTF cores are almost planar, contrary to the neutral form for which a twisted conformation is predicted, in agreement with the X-ray structure determinations. There are no direct experimental data available for the radical cations of this family of compound, but the calculations predict that the geometry of the radical cation is similar to that of the dication, confirming the occurrence of the largest structural changes at the level of the first oxidation step. This conclusion is largely supported by the RX structure of $\mathbf{4}^{\bullet+}$ (see Figure 3). Similar patterns are obtained when a withdrawing group is introduced on the phenyl ring, i.e., the neutral form is twisted when the radical cation and the dication display an almost planar TTF core (see Figure 4). The situation changes when a donor group is introduced on the phenyl ring and the dication is no longer planar. This change of behavior can be explained simply if we

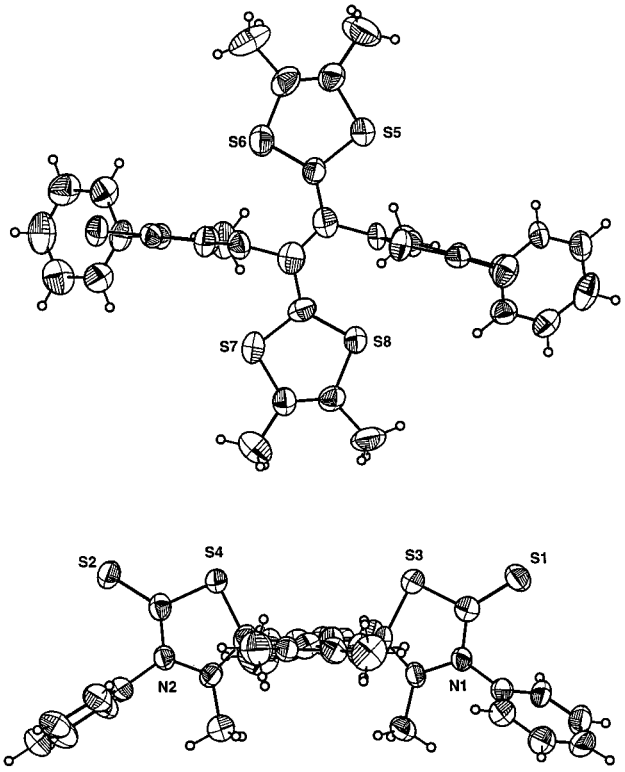

Figure 3. Crystal structure of compound **4** radical cation.

consider that the dication gets stabilized by conjugation with the phenyl ring bearing strong donor groups that stabilizes the positive charges. In the case of the simple phenyl and of course for withdrawing substituents, the dication has a better advantage to make the TTF core planar. On the contrary, in the case of the donor group substitution, there is a competition between the stabilization energy brought by the conjugation at the level of the TTF core and the energy gained by the stabilization of the positive charge by donor groups. However, in polar solvent, the electronic effects due to the repulsion of the two positive charges are lowered, and thus it is likely that the calculations of the conformations in gas phase overestimate the twisting of the TTF core in the dicationic state. One way to discuss the effects of the structural modifications on the relative order of potentials is to examine the changes in the energy orbital from where the second electron will be removed.[15a] In oxidation, the energy of the SOMO (single occupied orbital) of the radical cation is raised by the structural changes, resulting in an enhancement of the second electron removal compared to the first one. The analysis consists of calculating the difference ΔU_{SOMO} between the energy of the SOMO orbital of the radical cation in its optimized form and in the conformation of the neutral species. ΔU_{SOMO} values of 0.30, 0.35, 0.60, 0.63 eV were found for the unsubstituted **1** and the substituted TTF, **2d** (R═p-$MeOC_6H_4$), **2c** (R═C_6H_5) and **2b** (R═p-NCC_6H_4), respectively, meaning that the enhancement for the removal of the second electron is expected to vary in the order **2b** > **2c** > **2d** > **1**. Indeed the same experimental trend is observed for the inversion of potential, which confirms the idea that the structural changes are responsible for the potential inversion. It also indicates that most of the structure changes responsible for the potential inversion occur after the first electron transfer, as this approach does not take into account the possible structural changes occurring after the second electron transfer.[30] It is noticeable that apparently similar changes of structure lead to quite different changes of ΔU_{SOMO}. This can be explained quantitatively if we consider that the change of structure raises the energy of the SOMO but simultaneously lowers the conjugation with the phenyl substituent, leading to an opposite effect that is especially observable when a donor group is present on the phenyl ring or on the contrary to an additional effect in

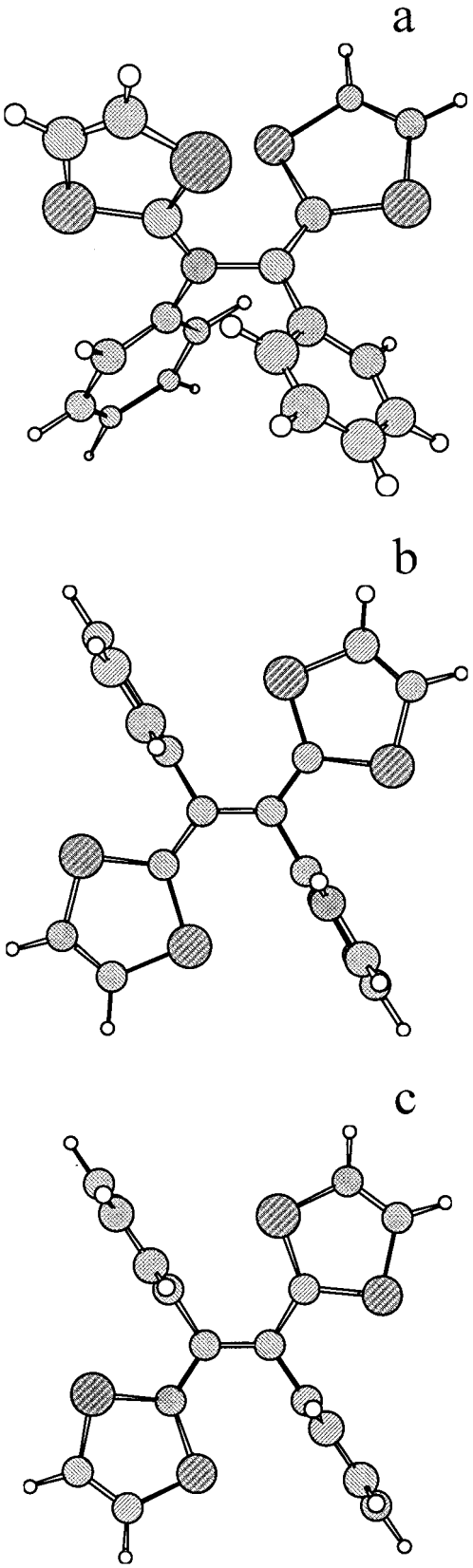

Figure 4. Optimized geometries calculated at the B3LYP/6-31G* level, of the neutral (a), radical cation (b), dication (c) of **2c** (R═C_6H_5).

TABLE 5: Calculated $\Delta U_{el,disp} + \Delta G^{\circ}_{solv,disp}$ in eV for the Investigated Dimers[a]

	R=	Gas Phase	in CH_2Cl_2	in CH_3CN
1	H	4.24	1.06	0.75
2d	p-$MeOC_6H_4$	3.45	0.88	0.61
2c	C_6H_5	3.58	0.81	0.53
2b	p-NCC_6H_4	3.42	0.72	0.43
3b	o-NCC_6H_4	3.59	0.85	0.56

[a] $\Delta U_{el,disp} + \Delta G^{\circ}_{solv,disp}$ = U_{el}(dication) + U_{el}(neutral) − 2*U_{el}(radical cation) + ΔG°_{solv}(dication) + ΔG°_{solv}(neutral) − 2*ΔG°_{solv}(radical cation).

the case of withdrawing substituents. If we do the same calculations for **3b** (R=o-NCC_6H_4), we found a ΔU_{SOMO} value of 0.65 eV from which we should expect a larger potential inversion for **3b** than for all the other compounds. Such a prediction is obviously in total disagreement with the experimental observations shown in Table 1. To understand this anomaly, it seems better to focus on the variations of the disproportionation free energies that are measurements of the radical cation stability and which take into account the structural changes associated with all of the redox states:

$$2TTF^{\bullet+} \rightleftarrows TTF^{2+} + TTF \qquad \Delta G^{\circ}_{disp}$$

The simplest approach is to compare the experimental data ΔG°_{disp} with the variation of the electronic energies for the disproportionation reaction $\Delta U_{el,disp}$. However, to be able to discuss the experimental variations of ΔG°_{disp}, we need a way to estimate the solvation free energies for each species, as much of this free energy in gas phase has an electrostatic origin. We used the IPCM method in which the solvent is described as a dielectric continuum using the conformations previously optimized in gas-phase calculations.[31] $\Delta U_{el,disp}$ were calculated as the differences between the electronic energies in gas phase. Thus $\Delta U_{el,disp} + \Delta G^{\circ}_{solv,disp} = U_{el(dication)} + U_{el(neutral)} - 2*U_{el(radical\ cation)} + \Delta G^{\circ}_{solv(dication)} + \Delta G^{\circ}_{solv(neutral)} - 2*\Delta G^{\circ}_{solv(radical\ cation)}$.[32] The calculated absolute values were always higher than the experimentally observed ΔG°_{disp}. If this overestimation was due in a large part to the simplifications used in the modeling,[31,32] other factors, such as the effect of ion-pairing with the anion of the supporting electrolyte, should also contribute to a decrease of the experimental ΔG°_{disp}.[27b] The calculated $\Delta U_{el,disp} + \Delta G^{\circ}_{solv,disp}$ values decrease when passing from the dichloromethane to the acetonitrile, as can be expected from lower repulsion energies between the two positive charges in a solvent with a higher dielectric constant. For the **1** and **2** series of compounds, the variation for the different substituents follows exactly the experimental variation for the potential inversion. The largest value is observed for the unsubstituted TTF vinylogue **1**, which displays experimentally the highest separation between the oxidation potentials. In the series of the phenyl-substituted compounds, the lowest $\Delta U_{el,disp} + \Delta G^{\circ}_{solv,disp}$ value is obtained for **2b** (R=p-NCC_6H_4) and the highest for **2d** (R=p-$MeOC_6H_4$) as found experimentally. From Table 5, we can observe that a compound for which $\Delta U_{el,disp} + \Delta G^{\circ}_{solv,disp}$ is higher than or equal to 0.6 eV displays two separated electron transfers, whereas an inverted potential situation occurs for $\Delta U_{el,disp} + \Delta G^{\circ}_{solv,disp} < 0.6$ eV. Let's now consider the effect of passing the substituent from the para position to the ortho position on the phenyl ring. A large increase of the experimental ΔG°_{disp} is expected in view of the DFT calculations (≈0.13 eV) between **2b** and **3b** even if the estimated increase is slightly lower than the experimental value (≈0.17 eV from Table 1). To explain the additional influence of the ortho position another way for understanding the inversion of potential is to focus on the energies of each individual species ($\Delta U_{el} + \Delta G^{\circ}_{solv}$) and to investigate how they vary with the introduction of the steric hindrance in the system. Compared to the unsubstituted TTF **1**, the presence of bulky substituents on the central TTF core destabilizes all of the redox forms because the planarity is more difficult to achieve. The destabilization energies have no reason to be the same for all of the redox species, resulting in different shifts for the first and second oxidation potentials. For compounds in the para series **2a**−**d**, the experimental E° and calculated $\Delta U_{el,disp} + \Delta G^{\circ}_{solv,disp}$ values show that the radical cation is more destabilized by the phenyl group than the two other redox states, which is responsible for the inversion or compression of potentials. Besides this effect, the ortho substituents create an additional destabilization due to the interactions between the ortho substituents and the TTF core. This additional effect has a considerable influence that can be estimated from the differences between the total electronic energies obtained from the B3LYP calculations. For example, in acetonitrile, the derived differences $(\Delta U_{el} + \Delta G^{\circ}_{solv})_{ortho} - (\Delta U_{el} + \Delta G^{\circ}_{solv})_{para}$ for the CN substituted TTF **3b** and **2b** are 0.25, 0.16, 0.20 eV for the neutral, radical cation and dication, respectively, confirming the idea of a higher destabilization ortho effect for the neutral and dication species. In acetonitrile (see Table 1), the ortho effect canceled completely the compression of potential, and in CH_2Cl_2, the ΔE° separation becomes even higher than for the unsubstituted TTF **1**. It results a situation where the changes of conformation do not lead to a compression as generally observed[12,14,15] but to an increase of ΔE°. The variation of the redox behavior with the ortho substituents is more difficult to rationalize than for the para substituents, because for each ortho group both electronic and steric effects are modified. However, we may expect a higher influence of the additional ortho steric influence of the o-NO_2 group that is bigger than the o-CN. Indeed, not only does **3a** display a higher ΔE° value in CH_2Cl_2 but also the neutral form is so destabilized that the o-NO_2-substituted compounds become easier to oxidize than the o-CN, contrary to their withdrawing properties.

Kinetics of the Electron Transfers. The previous experiments and modeling calculations allow us to predict the thermodynamics of the electron transfers, but they give little information about the timing or sequence of the different steps. Two limiting situations can be envisaged. In the first one, changes of conformation occur simultaneously with the electron transfers and we have an EE mechanism.

$$TTF \rightleftarrows TTF^{\bullet+} + e^- \qquad E^{\circ}_1,\ k_{s,1}$$

$$TTF^{\bullet+} \rightleftarrows TTF^{2+} + e^- \qquad E^{\circ}_2,\ k_{s,2}$$

The other limiting situation will be a stepwise mechanism: a radical cation similar to that of the neutral species is first produced, and then its conformation changes to give the more planar radical cation, resulting in a global ECE mechanism.[33] To address this point, we focused on the three previous molecules of series **2** with the para substituents on the phenyl ring and in acetonitrile. The first indication in favor of the EE mechanism is obtained from the fact that no intermediate can be detected from cyclic voltammetry up to several thousands volts per second, corresponding to experimental times in the tenths of millisecond. Another indication comes from the molecular modeling where it was not possible to find another

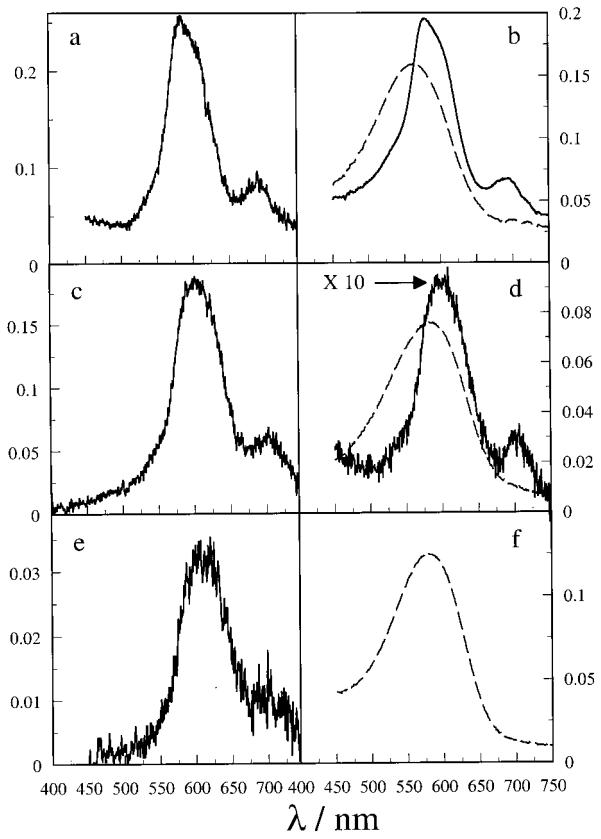

Figure 5. UV−visible spectra of the radical cations and dications of **1** (a), **2d** (b), **2c** (c) produced by flash photolysis (a, b, c) in acetonitrile + 1% CCl_4 and recorded just after the laser flash (50−100 ns). Comparison with the electrochemical oxidation (b, d, f) in acetonitrile (single spectra from Figure 3), radical cation (—), dication (- - -).

stable conformation more similar to the neutral species. To go to shorter experimental times, the radical cation was produced by flash photolysis of a solution of TTF in the presence of 1% CCl_4 under air acting as an electron scavenger:[34]

$$TTF \xrightarrow{h\nu} TTF^{\bullet+} + CCl_3^{\bullet} + Cl^-$$

$$CCl_3^{\bullet} + O_2 \rightarrow CCl_3O_2^{\bullet}$$

$$CCl_3O_2^{\bullet} + TTF \rightarrow CCl_3O_2^- + TTF^{\bullet+}$$

Differential UV−visible spectra recorded just after the laser pulse (50−100ns) are shown in Figure 5 and are compared with the spectra recorded during spectroelectrochemical experiments (experimental time 1s). It is clearly visible that similar spectra are observed in both methods,[35] and they show that the same final radical cations are already produced for times shorter than 50−100 ns after the pulse.

In experimental situations of inverted potentials, the reported rates of heterogeneous electron transfers are generally rather slow with large separations between the forward and the reverse peak potentials (large ΔE_p)[12,14,15] because, in the framework of an EE mechanism, the reorganization energy related the structural changes contributes to the activation barrier. For our TTF vinylogues, the simple examination of the voltammograms (thin shape peaks, small peak to peak potential separation) shows that the global electron process is fast.[36] More precise kinetics data and measurements of standard heterogeneous electron-transfer kinetics constants can be derived from the variations of the peak potentials with the scan rates. For the unsubstituted compound **1**, two monoelectronic waves are observed regardless of the scan rate. From the analysis of the voltammograms recorded in the 1000−5000 V s^{-1} range, we estimated values of 3−4 and 1.5 cm s^{-1} for the electrochemical standard rates for the first ($k_{s,1}$) and second ($k_{s,2}$) electron transfers (uncorrected from the double layer effect and taking a value of $\alpha = 0.5$ for the transfer coefficient[37]). For **2b** and **2d**, only one bielectronic process is observed, and as we have done in the preliminary treatment of Table 1, the peak separation recorded at low scan rates can be used to measure the two redox potentials if the thermodynamic control is reached. The thermodynamic control situation can be checked from the invariance of the oxidation peak potential with the lowest scan rates.[27] This is clearly the case for **2d**, and we deduced $E_1^\circ = 0.376$ and $E_2^\circ = 0.380$ V/SCE. When the E° values are known, the value of $k_{s,1}$ can easily be estimated from the variation of the oxidation peak potential $E_{p,ox}$ with the scan rate.[38] Rigorously, the value of $E_{p,ox}$, and thus of the value estimated for $k_{s,1}$ depends on the rate of the second electron transfer. Because the conformational change is much larger for the first electron transfer than for the second one, $k_{s,2}$ is expected to be larger than $k_{s,1}$. Considering the two limiting cases where $k_{s,1} = k_{s,2}$ and $k_{s,2} = 5$ cm s^{-1} (the highest values of k_s found for an aromatic molecule),[39] we deduced that $k_{s,1}$ ranges from 1.5−2.0 cm s^{-1}. The kinetics situation is less favorable for the CN compound **2d** for which a ΔE_p value of 30 mV is obtained, meaning that it is difficult to extract precise values for the two E°. Moreover, the variations of the peak potentials with the scan rate indicate an influence of the electron-transfer kinetics, even for the measurements performed at the lowest scan rates (see Figure 6). By comparison of simulations corresponding to an EE mechanism with the experimental data,[40] we found that the best agreement was obtained for $E_1^\circ = 0.580$ V, $E_2^\circ = 0.481$ V ($\Delta E^\circ = 0.1$ V),[41] $k_{s,1} = 0.6$ cm s^{-1}, $k_{s,2} = 3$ cm s^{-1}, but similar results were obtained for $\Delta E^\circ = 0.15$ and $k_{s,1} = 1$ cm s^{-1}.

In the framework of the Marcus−Hush model,[42] the reorganization free energy of the electron transfer λ_{elec} is divided into a solvent reorganization term, $\lambda_{0,elec}$, and an intramolecular reorganization term, $\lambda_{i,elec}$, where $\lambda_{elec} = \lambda_{0,elec} + \lambda_{i,elec}$. The electrochemical reorganization energies may themselves be derived from the previously determined electrochemical standard rate constants, k_s. As shown from data on the electrochemical reduction of a series of aromatic molecules,[43] a good comparison of λ_{elec} with theoretical predictions can be obtained from k_s values that are uncorrected for double-layer effect and using Hush's model for $\lambda_{o,elec}$ where image effect is not taken into account[42c,d] due to a cancellation of these two effects.[44] Thus, estimations were made according to the following equations:[44b]

$$k_s = Z^{el} \exp\left[-\frac{F(\lambda_{0,elec} + \lambda_{i,elec})}{4RT}\right]$$

$$\text{with } Z^{el} = \sqrt{\frac{RT}{2\pi M}} \quad (M, \text{ molar mass})$$

$$\text{and } \lambda_{0,elec} = 3/a \quad (a, \text{ radius of the equivalent sphere in Å})$$

In this case, $\lambda_{i,elec}$ can be estimated[45] from the difference in energy between the neutral TTF at its equilibrium geometry and at the equilibrium geometry of the radical cation (λ_1) and conversely, from the difference in energy between the radical cation at its equilibrium geometry and at the equilibrium geometry of the neutral TTF (λ_2).[45d,46] When these two energies

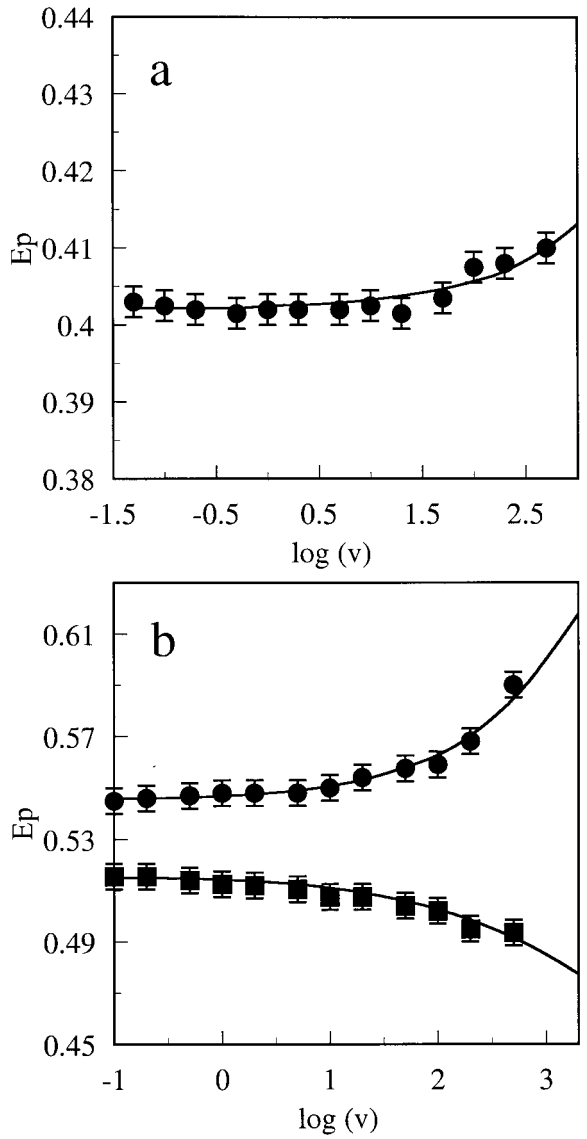

Figure 6. Cyclic voltammetry in acetonitrile (+ 0.1 mol L^{-1} of NEt_4BF_4), 1 mm Pt electrode. Temp = 20 °C. (a) Oxidation of **2d** (R= p-$MeOC_6H_4$). Conc = 6×10^{-4} mol L^{-1}. Variation of the oxidation peak potential with the scan rate. The line is the theoretical variation for $k_{s,1} = 1.5$ cm s^{-1}, $k_{s,2} = 5$ cm s^{-1}. (b) Oxidation of **2b**. Variations of the oxidation (●) and reduction (■) peak potentials with the scan rate. (R=p-NCC_6H_4). Conc = 4.5×10^{-4} mol L^{-1}. Lines are the simulated values for $E_1^\circ = 0.580$ V, $E_2^\circ = 0.481$ V, $k_{s,1} = 0.6$ cm s^{-1}, $k_{s,2} = 3$ cm s^{-1}.

are not equal, and assuming a parabolic energy-reaction coordinate dependence, $\lambda_{i,elec}$ can be approximated by[46]

$$\lambda_{i,elec} = \lambda_1 \left[\frac{1 - \sqrt{\frac{\lambda_1}{\lambda_2}}}{1 - \frac{\lambda_1}{\lambda_2}} \right]^2$$

Experimental and theoretical values for the activation barriers are gathered in Table 7. Even if the experimental $k_{s,1}$ values must be considered as approximate, the comparison of the experimental data with theoretical parameters shows a good agreement with the occurrence of an EE mechanism in which the electron transfer is concerted with the conformation changes. The interesting feature of these systems is that, despite the large configuration changes associated to the electron transfers, the intrinsic barriers remain relatively low.

TABLE 6: Maximum Absorption Wavelengths in CH_3CN (in nm)

	R	neutral	radical cation	dication
1	H	386, 404	579, 690[a,b]	564[b]
2b	p-NCC_6H_4	393	610, 700[a]	581[b]
2d	p-$MeOC_6H_4$	335	601, 700[a,b]	585[b]
3b	o-NCC_6H_4	317, 370 (S)	617, 700[b]	600[b]
3d	o-$MeOC_6H_4$	290, 355[c]	589, 700[b]	584[b]

[a] Flash photolysis. [b] Spectroelectrochemistry. (S) Shoulder.

TABLE 7: Experimental and Theoretical Kinetics Parameters for the First Electron Transfer

		exptl			theor		
	R =	$k_{s,1}$[a]	λ_{elec}[b]	a[c]	$\lambda_{0,elec}$[b]	$\lambda_{i,elec}$[b]	λ_{elec}[b]
1	H	4−3	0.679−0.708	5.59	0.536	0.163	0.699
2b	p-NCC_6H_4	1−0.5	0.796−0.867	6.51	0.460	0.436	0.896
2d	p-$MeOC_6H_4$	2.0−1.5	0.726−0.755	6.62	0.453	0.347	0.800

[a] In cm s^{-1}. [b] Energies in eV. [c] Radii in Å.

Conclusion

The oxidation of these TTF vinylogues is another example of electron transfer reaction where the electron transfers are associated with large structural changes. Through fine-tuning of the molecular structure (control of the steric hindrance) and substituent choice, it is possible to control the relative stabilities of the different redox species. At one end, this leads to situations of compression of potential where the second electron transfer is much easier than the first one. At the other end, opposite situations are obtained with a large increase of the separation between the first and second oxidation potentials compared to a similar TTF vinylogue without steric hindrance. Therefore, paramagnetic radical cation can be isolated for the design of solid-state compounds blessed with the collective electronic properties. Interestingly for the engineering of new materials using the molecular movement, the inner reorganization energies remain modest (0.35−0.45 eV), allowing a fast passage between the different conformations during the electron transfers.

Acknowledgment. The authors thank Dr. Philippe Guiriec (Université Denis Diderot-Paris 7) for his help in the spectroelectrochemical experiments.

References and Notes

(1) (a) Université de Rennes 1. (b) Institut des Matériaux de Nantes. (c) Université Denis Diderot-Paris 7.

(2) (a) Yoshida, Z.; Kawase, T.; Awaji, H.; Sugimoto, I.; Sugimoto, T.; Yoneda, S. *Tetrahedron Lett.* **1983**, *24*, 3469. (b) Sugimoto, T.; Awaji, H.; Sugimoto, I.; Misaki, Y.; Kamase, T.; Yoneda, S.; Yoshida, Z.; Kobayashi, T.; Anzai, H. *Chem. Mater.* **1989**, *1*, 535. (c) Hansen, T. K.; Lakshmikantham, M. V.; Cava, M. P.; Metzger, R. M.; Becher J. *J. Org. Chem.* **1991**, *56*, 2720. (d) Moore, A. J.; Bryce, M. R.; Ando, D. J.; Hursthouse, M. B. *J. Chem. Soc., Chem. Commun.* **1991**, 320. (e) Moore, A. J.; Bryce, M. R. *Tetrahedron Lett.* **1992**, *33*, 1373. (f) Bryce, M. R.; Coffin, M. A.; Clegg, W. *J. Org. Chem.* **1992**, *57*, 1696. (g) Bryce, M. R.; Moore, A. J.; Tanner, B. K.; Whitehead, R.; Clegg, W.; Gerson, F.; Lamprecht, A.; Pfenninger, S. *Chem. Mater.* **1996**, *8*, 1182.

(3) See for example Schukat, G.; Fanghänel, E. *Sulfur Reports* **1996**, *18*, 1.

(4) (a) Kirmse, W.; Horner, L. *Liebigs Ann. Chem.* **1958**, *614*, 4. (b) Mayer, K.; Kröber, H. *J. Prakt. Chem.* **1974**, *316*, 907. (c) Cava, M. P.; Lakshmikantham, M. V. *J. Heterocycl. Chem.* **1980**, *17*, S39. (d) Schöberl, U.; Salbeck, J.; Daub, J. *Adv. Mater.* **1992**, *4*, 41.

(5) (a) Lorcy, D.; Carlier, R.; Robert, A.; Tallec, A.; Le Maguerès, P.; Ouahab, L. *J. Org. Chem.* **1995**, *60*, 2443. (b) Hapiot, P.; Lorcy, D.; Carlier, R.; Tallec, A.; Robert, A. *J. Phys. Chem.* **1996**, *100*, 14823. (c) Benahmed-Gasmi, A.; Frère, P.; Roncali, J.; Elandaloussi, E.; Orduna, J.; Garin, J.;

Jubault, M.; Gorgues, A. *Tetrahedron Lett.* **1995**, *36*, 2983. (d) Bellec, N.; Lorcy, D.; Robert, A.; Carlier, R.; Tallec, A. *J. Electroanal. Chem*. **1999**, *462*, 137.

(6) (a) Ohta, A.; Yamashita, Y. *J. Chem. Soc., Chem. Commun.* **1995**, 1761. (b) Yamashita, Y.; Tomura, M.; Braduz Zaman, M.; Imaeda, K. *J. Chem. Soc., Chem. Commun.* **1998**, 1657.

(7) Moore, A. J.; Bryce, M. R.; Skabara, P. J.; Batsanov, A. S.; Goldenberg, L. M.; Howard, J. A. K. *J. Chem. Soc., Perkin Trans. 1* **1997**, 3443.

(8) Hascoat, P.; Lorcy, D.; Robert, A.; Carlier, R.; Tallec, A.; Boubekeur, K.; Batail, P. *J. Org. Chem.* **1997**, *62*, 6086.

(9) Fourmigué, M.; Johannsen, I.; Boubekeur, K.; Nelson, C.; Batail, P. *J. Am. Chem. Soc.* **1993**, *115*, 3752.

(10) Gonzalez, S.; Martin, N.; Sanchez, L.; Segura, J. L.; Seoane, C.; Fonseca, I.; Cano, F. H.; Sedo, J.; Vidal-Gancedo J.; Rovira, C. *J. Org. Chem*. **1999**, *64*, 3498.

(11) Hopf, H.; Kreutzer, M.; Jones, P. G. *Angew. Chem., Int. Ed. Engl.* **1991**, *30*, 1127.

(12) (a) Evans, D. H.; O'Connell, K. M. Conformational Change and Isomerization Associated with Electrode Reactions. In *Electroanalytical Chemistry*; Bard, A. J., Ed.; Marcel Dekker: New York, 1986; Vol. 14, pp 113−207. (b) Evans, D. H.; Lehmann, M. W. *Acta Chem. Scand*. **1999**, *53*, 765.

(13) (a) Yoshida, Z.-I.; Kawase, T.; Awaji, H.; Yoneda, S. *Tetrahedron Lett.* **1983**, *24*, 3469. (b) Benahmed-Gasmi, A.; Frère, P.; Elandaloussi, E. H.; Roncali, J.; Orduna, J.; Garin, J.; Jubault, M.; Riou, A.; Gorgues, A. *Chem. Mater*. **1996**, *8*, 2291. (c) Moore, A. J.; Bryce, M. R.; Batsanov, A. S.; Green, A.; Howard, J. A. K.; Mckervey, A.; Mcguigan, P.; Ledoux, I.; Ortí, E.; Viruela, R.; Viruela, P. M.; Tarbit B. *J. Mater. Chem.* **1998**, *8*, 1173. (d) Roncali, J. *Acc. Chem. Res.* **2000**, *33*, 147.

(14) Evans, D. H.; Hu, K. *J. Chem. Soc., Faraday Trans*. **1996**, *92*, 3983.

(15) (a) Hu, K.; Evans, D. H. *J. Phys. Chem.* **1996**, *100*, 3030. (b) Hu, K.; Evans, D. H. *J. Electroanal. Chem.* **1997**, *423*, 29. (c) Speiser, B.; Würde, M.; Maichle-Mössmer, C. *Chem. Eur. J.* **1998**, *4*, 222. (d) Dümmling, S.; Speiser, B.; Kuhn, N.; Weyers *Acta Chem. Scand.* **1999**, *53*, 876.

(16) (a) Lorcy, D.; Le Maguerès, P.; Rimbaud, C.; Ouahab, L.; Delhaes, P.; Carlier, R.; Tallec, A.; Robert, A. *Synth. Met.* **1997**, *86*, 1831. (b) Rimbaud, C.; Le Maguerès, P.; Ouahab, L.; Lorcy, D.; Robert, *Acta Crystallogr.* **1998**, *C54*, 679.

(17) Garreau, D.; Savéant, J.-M. *J. Electroanal. Chem*. **1972**, *35*, 309.

(18) Andrieux, C. P.; Garreau, D.; Hapiot, P.; Pinson, J.; Savéant, J.-M. *J. Electroanal. Chem*. **1988**, *243*, 321.

(19) (a) Neudeck, A.; Dunsch, L. *J. Electroanal. Chem*. **1994**, *370*, 17. (b) Neudeck, A.; Dunsch, L. *J. Electroanal. Chem*. **1995**, *386*, 138. (c) Neudeck, A.; Dunsch, L. *Electrochimica. Acta* **1995**, *40*, 1427.

(20) Rudolph, M.; Reddy, D. P.; Felberg, S. W. *Anal. Chem.* **1994**, *66*, 589A.

(21) Frisch, M. J.; Trucks, G. W.; Schlegel, H. B.; Scuseria, G. E.; Robb, M. A.; Cheeseman, J. R.; Zakrzewski, V. G.; Montgomery, J. A., Jr.; Stratmann, R. E.; Burant, J. C.; Dapprich, S.; Millam, J. M.; Daniels, A. D.; Kudin, K. N.; Strain, M. C.; Farkas, O.; Tomasi, J.; Barone, V.; Cossi, M.; Cammi, R.; Mennucci, B.; Pomelli, C.; Adamo, C.; Clifford, S.; Ochterski, J.; Petersson, G. A.; Ayala, P. Y.; Cui, Q.; Morokuma, K.; Malick, D. K.; Rabuck, A. D.; Raghavachari, K.; Foresman, J. B.; Cioslowski, J.; Ortiz, J. V.; Stefanov, B. B.; Liu, G.; Liashenko, A.; Piskorz, P.; Komaromi, I.; Gomperts, R.; Martin, R. L.; Fox, D. J.; Keith, T.; Al-Laham, M. A.; Peng, C. Y.; Nanayakkara, A.; Gonzalez, C.; Challacombe, M.; Gill, P. M. W.; Johnson, B. G.; Chen, W.; Wong, M. W.; Andres, J. L.; Head-Gordon, M.; Replogle, E. S.; Pople, J. A. *Gaussian 98*, revision A.1; Gaussian, Inc.: Pittsburgh, PA, 1998.

(22) Becke, A. D. *J. Chem. Phys.* **1993**, *98*, 5648.

(23) Hariharan, P. C.; Pople, J. A. *Chem. Phys. Lett*. **1972**, *16*, 217.

(24) (a) Hybrid density functional methods with the 6-31G* base have been used previously for calculations on neutral and radical cation of hetorocycles containing sulphur atoms[24b] and on extended TTF and found to give a good qualitative description of properties. (b) See for example references 24c, 24d, and 13c. (c) Hernández, V.; Muguruma, H.; Hotta, S.; Casado, J.; López Navarrete, J. T. *J. Phys. Chem. A* **2000**, *104*, 735. (d) Keszthelyi, T.; Grage, M. M.-L.; Offersgaard, J. F.; Wilbrandt, R.; Svendsen C.; Mortensen, O. S.; Pedersen, J. K.; Jensen, H. J. A. *J. Phys. Chem. A* **2000**, *104*, 2808.

(25) (a) Foresman, J. B.; Keith, T. A.; Wiberg, K. B.; Snoonian, J.; Frisch, M. J. *J. Phys. Chem.* **1996**, *100*, 16098. (b). For a general review about solvation methods see: Cramer, J.; Truhlar, D. G. *Chem. Rev.* **1999**, *99*, 2161.

(26) When two close waves were observed, the same equation was used with $E^\circ_{2e^-} = (E_{pa,2} + E_{pc,1})/2$ where $E_{pa,2}$ and $E_{pc,1}$ are for the second and first oxidation peak potentials, respectively.

(27) (a) Myers, R. L.; Shain, I. *Anal. Chem.* **1969**, *41*, 980. (b) Andrieux, C. P.; Savéant, J.-M. *J. Electroanal. Chem.* **1974**, *57*, 27.

(28) The value of the disproportionation equilibrium constant K is given by equation $K = \exp\{(E^\circ_1 - E^\circ_2)F/RT\}$.

(29) The authors have deposited atomic coordinates for this structure with the Cambridge Crystallographic Data Centre. The coordinates can be obtained, on request, from the Director, Cambridge Crystallographic Data Centre, 12 Union Road, Cambridge, CB2 1EZ, U.K.

(30) Agreement between theoretical expectations and experiments are expected if the structural reorganizations occurring at the level of the second electron transfer for the compounds of **2** have negligible or similar influence.

(31) We are aware that the conformations (especially of the dication species) in the presence of a solvent can be slightly changed from the optimization made in the gas phase. However, optimization in the presence of solvent would have required unrealistic calculation times. This approach was chosen as a compromise between calculation time and precision.

(32) The relative variations of $\Delta U_{el,disp} + \Delta G^\circ_{solv,disp}$ in the same family of compounds provide interesting information when compared to the experimental values of ΔG°_{disp}. We can expect that for a comparison inside the same family of molecules, the differences of thermal and ZPE corrections between the neutral, radical cation, and dication corresponding to the disproportionation reaction will not change much, meaning a similar trend between ΔG°_{disp} and $\Delta U_{el,\ disp} + \Delta G^\circ_{solv,disp}$.

(33) Savéant, J.-M.; Andrieux, C. P.; Nadjo, L. *J. Electroanal. Chem*. **1973**, *41*, 137.

(34) See for example: Guyard, L.; Hapiot, P.; Neta, P. *J. Phys. Chem. B* **1997**, *101*, 5698.

(35) One possible question concerns the assignment of the absorption bands for the radical cation because radical cations of TTF have a high propensity to reversibly dimerize ("π-dimer").[35b] The similarity between the spectra recorded in flash photolysis and spectroelectrochemical experiments confirmed that the spectra correspond to the radical cations and not to dimers. The concentrations of produced radical cation are typically in the range of a few micromolar in flash photolysis against a millimolar in spectroelectrochemistry. Moreover, considering the bulky substituents and thus the important interplanar separation between successive extended TTF cores, dimerization of radical cations appears to be very unfavorable. (b) Levillain, E.; Roncali; J. *J. Am. Chem. Soc.* **1999**, *121*, 8760.

(36) Evans, D. H. *Acta Chem. Scand.* **1998**, *52*, 194 and references therein.

(37) (a) The use of the Buttler−Volmer law and of a value $\alpha = 0.5$ for the transfer coefficient are justified under our experimental conditions because the differences between the peak potentials and the E° remain small (lower than 100 mV).[37b] Tests performed with Digisim 2.1 and the Marcusian kinetics instead of the Butler−Volmer law lead to negligible differences (lower than 1 mV on the calculated peak potentials). (b) Savéant, J.-M.; Tessier, D. *Faraday Discuss. Chem. Soc*. **1982**, *74*, 57.

(38) Andrieux, C. P.; Savéant, J.-M. Electrochemical reactions. In *Investigations of Rates and Mechanisms*; Bernasconi, C. F., Ed.; Wiley: New York, 1986; Vol. 6, 4/E, Part. 2, pp 305−390.

(39) Andrieux, C. P.; Hapiot, P.; Savéant, J.-M. *Chem. Rev.* **1990**, *112*, 2439.

(40) Homogeneous electron transfers have been considered in the simulations, and a value of $k = 10^8$ L mol^{-1} s^{-1} has been used. The choice of this value in the range 10^6−10^9 L mol^{-1} s^{-1} has been found to have very little influence on the simulation.

(41) The extracted potential values are more inverted that the values of Table 1 because the influence of electron-transfer kinetics has been neglected in the simple treatment of Table 1. Table 1 values have to be considered as a higher border for ΔE° values.

(42) (a) Marcus, R. A. *J. Chem. Phys.* **1956**, *24*, 966. (b) Marcus, R. A. *J. Chem. Phys*. **1956**, *24*, 979. (c) Hush, N. S. *J. Chem.Phys*. **1958**, *28*, 962. (d) Hush, N. S. *Trans. Faraday Soc*. **1961**, *57*, 557. (e) Marcus, R. A. J. *Chem. Phys*. **1965**, *43*, 679.

(43) Kojima H.; Bard, A. J. *J. Am. Chem. Soc*. **1975**, *97*, 6317.

(44) k_s values that are uncorrected for double layer effects lead to estimations of λ_{elec} that are slightly smaller than Hush's predictions.[44b] (b) Andrieux, C. P.; Savéant, J.-M.; Tardy, C. *J. Am. Chem. Soc*. **1998**, *120*, 4167.

(45) (a) For more general discussions and comparison about methods for estimating intramolecular reorganization energies, see for example refs 45b−e and references therein. (b) Mikkelsen, K. V.; Pedersen, S. U.; Lund, H.; Swanstrom, P. *J. Phys. Chem.* **1991**, *95*, 8892. (c) Eberson, L.; Gonzalez-Luque, Lorentzon J.; Merchan M.; Roos, B. O. *J. Am. Chem. Soc.* **1993**, *115*, 2898. (d) Klimkans, A.; Larsson, S. *Chem. Phys.* **1994**, *189*, 25. (e) Jakobsen, S. Mikkelsen, K. V.; Pedersen, S. U. *J. Phys. Chem*. **1996**, *100*, 7411.

(46) Brielbeck, B.; Rühl, J. C.; Evans, D. H. *J. Am. Chem. Soc.* **1993**, *115*, 11898.